Medical Image Analysis with Artificial Neural Networks

J. Jiang, P. Trundle and J. Ren
Digital Media & Systems Research Institute, University of Bradford,
Bradford, BD7 1DP, United Kingdom
Email: (j.jiang1, p.r.trundle, j.ren)@bradford.ac.uk

ABSTRACT: *Given that neural networks have been widely reported in the research community of medical imaging, we provide a focused literature survey on recent neural network developments in computer-aided diagnosis, medical image segmentation and edge detection toward visual content analysis, and medical image registration for its pre-processing and post processing, with the aims of increasing awareness of how neural networks can be applied to these areas and to provide a foundation for further research and practical development. Representative techniques and algorithms are explained in detail to provide inspiring examples illustrating: (i) how a known neural network with fixed structure and training procedure could be applied to resolve a medical imaging problem; (ii) how medical images could be analysed, processed, and characterised by neural networks; and (iii) how neural networks could be expanded further to resolve problems relevant to medical imaging. In the concluding section, a highlight of comparisons among many neural network applications is included to provide a global view on computational intelligence with neural networks in medical imaging.*

Indexing terms: *neural networks, medical imaging analysis, and intelligent computing.*

1. Introduction

Inspired by the way biological nervous systems such as human brains process information, an artificial neural network (ANN) is an information processing system which contains a large number of highly interconnected processing neurons. These neurons work together in a distributed manner to learn from the input information, to coordinate internal processing, and to optimise its final output. As numerous algorithms have been reported in the literature applying neural networks to medical image analysis, we provide a focused survey on computational intelligence with neural networks covering medical image registration, segmentation and edge detection for medical image content analysis, computer-aided detection and diagnosis with specific coverage on mammogram analysis towards breast cancer screening, and other applications providing a global view on the variety of neural network applications and their potential for further research and developments.

Neural network applications in computer-aided diagnosis represent the main stream of computational intelligence in medical imaging [1-14]. Their penetration and involvement are almost comprehensive for all medical problems due to the fact that neural networks have the nature of adaptive learning from input information and, using a suitable learning algorithm, can improve themselves in accordance with the variety and the change of input content. Furthermore, neural networks have the capability of optimising the relationship between the inputs and outputs via distributed computing, training, and processing, leading to reliable solutions desired by specifications, and medical diagnosis often relies on visual inspection, and medical imaging provides the most important tool for facilitating such inspection and visualization.

Medical image segmentation and edge detection remains a common problem and foundational for all medical imaging applications [15-25]. Any content analysis and regional inspection requires segmentation of featured areas, which can be implemented via edge detection and other techniques. Conventional approaches are typified by a range of well researched algorithms, including watershed [15], snake modelling [16] and region-growing [17]. In comparison, neural network approaches exploit the learning capability and training mechanism to classify medical images into content consistent regions to complete segmentations as well as edge detections [23-25].

Another fundamental technique for medical imaging is registration, which plays important roles in many areas of medical applications [26-32]. Typical examples include wound care, health care surveillance and monitoring etc. Neural networks can be designed to provide alternative solutions via competitive learning, self-organising and clustering to process input features and find the best possible alignment between different images or data sets.

Other applications of ANN include data compression [33-38], image enhancement and noise suppression [39-44], and disease prediction [45, 46] etc. More recently, application of ANN for functional magnetic resonance imaging (MRI) simulation becomes a new research hotspot, where certain structured ANNs are employed to simulate the functional connectivity of brain networks [47, 48]. Due to the similar nature of ANN and human neurons, ANN has been proved to be a very useful for this new task [49, 50].

To provide useful insights for neural network applications in medical imaging and computational intelligence, we structure the rest of this paper in six further sections, where Section 2 provides some basics about neural networks to enable beginners to understand the structure, the connections, and the neuron functionalities. The next four sections present examples of using ANNs for medical imaging problems, categorised by their primary application area. Each section covers an application area that differs significantly from the others and groups together ANN examples that attempt to solve particular domain sub-problems. Furthermore, these sections are ordered to present applications in a way that naturally follows the flow of multiple pre-processing steps, such as registration and segmentation, through to endpoint applications performing real diagnostic tasks. Section 3 presents examples of image registration approaches. Section 4 covers image segmentation and edge detection techniques. Section 5 describes applications of computer aided diagnosis. Section 6 includes other applications that are not covered in the previous sections. Finally, conclusions and discussions are presented in section 7.

2. Neural Networks Fundamentals

To enable understanding of neural networks, facilitating possible repetition of those neural networks introduced and successfully applied in medical imaging, and to inspire further development of neural networks, we cover essential basics in this. We start from a theoretical model of a single neuron and then introduce a range of different types of neural networks to reveal their structure, training mechanism, operation, and functions.

2.1 Basic Structure

The basic structure of a neuron can be theoretically modelled as shown in Figure 1, where X {x_i, i = 1, 2, …, n} represent the inputs to the neuron and Y represents the output. Each input is multiplied by its weight w_i, a bias b is associated with each neuron and their sum goes through a transfer function f. As a result, the relationship between input and output can be described as follows.

$$Y = f\left(\sum_{i=1}^{n} w_i x_i + b\right) \qquad (1)$$

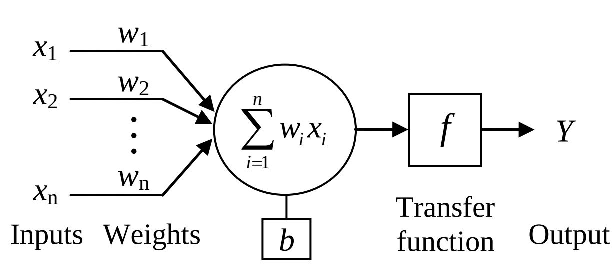

Figure 1 The model of a neuron

There are a range of transfer functions available to process the weighted and biased inputs, among which four basic transfer functions widely adopted for medical image processing are illustrated in Figure 2.

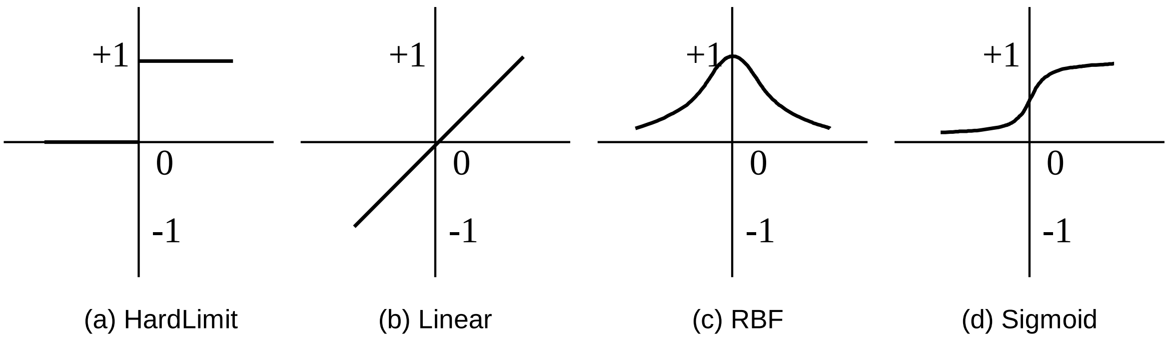

Figure 2 *Four widely adopted transfer functions*

Via selection of suitable transfer functions and connection of neurons, various neural networks can be constructed to be trained for producing the specified outputs. The learning paradigms for neural networks in medical image processing generally include supervised learning and unsupervised learning. In supervised learning, a network is trained using a set of inputs and outputs (targets). For each training case there will be a set of input values and one or more associated output values, and the goal is minimise the network's overall output error for all training cases by iteratively adjusting the neuron connection weights and bias values using a specific training algorithm.

In unsupervised learning, the training data set does not include any target information. Normally a function is defined that measures the suitability or accuracy of the network. This function, often referred to as a cost function, is dependent on the network's application and normally uses both the input values and the network's output value(s) to produce a cost for the current network configuration. Normally the aim of unsupervised learning is to minimise or maximise the cost for all input vectors in the training set.

2.2 Feed-forward Network

There are several different neural network architectures available for medical imaging applications, but one of the most common is the feed-forward network. In a feed-forward network, the neurons in each layer are only connected with the neurons in the next layer. These connections are unidirectional, which means signals or information being processed can only pass through the network in a single direction, from the input layer, through the hidden layer(s) to the output layer.

Feed-forward networks commonly use the Back-Propagation (BP) supervised learning algorithm to dynamically alter the weight and bias values for each neuron in the network. The algorithm works by iteratively altering the connection weight values for neurons based on the error in the network's actual output value when compared to the target output value. The actual modification of weights is carried out using a (normally stochastic) gradient descent algorithm, where the weights are modified after each training example is present to the network.

A Multilayer Perceptron (MLP) is a special type of feed-forward network employing three or more layers, with nonlinear transfer functions in the hidden layer neurons. MLPs are able to associate training patterns with outputs for nonlinearly separable data. Feed-forward networks are particularly suitable for applications in medical imaging where the inputs and outputs are numerical and pairs of input/output vectors provide a clear basis for training in a supervised manner.

2.3 Radial Basis Function Networks

A radial basis function (RBF) network is a three-layer supervised feed-forward network that uses a nonlinear transfer function (normally Gaussian) for the hidden neurons and a linear transfer function for the output neurons. The Gaussian function is applied to the net input of each neuron to produce a radial function of the distance between each pattern vector and each hidden unit weight vector.

RBF networks are inherently flexible in terms of their size and topology, making them suitable for a variety of problems. RBF networks have been successfully applied to a number of visual processing and analysis problems, including analysis of 3D structures, as well as time-series data. They have the potential to be useful tools for medical image analysis, and their application to medical imaging analysis problems is discussed further in section 3.2 and 5.1.

2.4 Feed-back Network

A feed-back (or recurrent) neural network can have signals travelling in both directions by introducing loops, propagating values from the hidden and output layers backwards to earlier layers. Their state changes continuously until they reach an equilibrium point. They remain at the equilibrium point until the input changes and a new equilibrium needs to be found. They are potentially powerful processing tools but can become extremely complicated.

A Hopfield network is a specific type of feedback network designed to act as a form of associative memory, in a similar way to certain parts of the human brain. The purpose of associative memory is to converge to a state remembered from training when only part of the state is presented as an input. The Hopfield network has no special input or output neurons; all neurons are both input and output, and all are connected to every other neuron in both directions. After receiving the input simultaneously by all the neurons, they output to each other continuously until a stable state is reached. In a Hopfield network, it is simple to set up the weights between neurons in order to attempt to set up a desired set of patterns as stable class patterns. They are potentially useful for medical imaging applications such as tumour classification where the output value (e.g. benign or malignant) must be derived from partial or similar patterns to those seen during training.

2.5 Self-Organising Map

Quite different from the above networks types, a Kohonen Neural Network or Self-Organising Map (SOM) learns to map input values to an (often two-dimensional) output space. SOMs maintain the topology of the input data while reducing the dimensionality, making them particularly useful for visualisation problems. SOMs can also be especially useful for medical imaging applications such as edge detection and segmentation, as their ability to automatically organise their neuron structures based on the topographical structure of the inputs can serve either as a first step in an algorithm incorporating many different approaches, or as a stand-alone method of dimensionality reduction and pattern recognition.

In a Kohonen neural network, each neuron is fed by input vector (data point) x $\in R^n$ through a weight vector w $\in R^n$. Each time a data point is input to the network, only the neuron j whose weight vector most resembles the input vector is selected to fire, according to the following rule:

$$j = \arg\min(\|x - w\|^2), \quad i = 1,2, .. \, m \qquad (2)$$

The firing or winning neuron j and its neighbouring neurons i have their weight vectors w modified according to the following rule:

$$w_i(t+1) = w_i(t) + h_{ij}(\|r_i - r_j\|, t) \cdot (x(t) - w_i(t)) \qquad (3)$$

Where $h_{ij}(\|r_i - r_j\|, t)$ is a kernel defined on the neural network space as a function of the distance $\|r_i - r_j\|$ between the firing neuron j and its neighbouring neurons i, and the time t here defines the number of iterations. Its neighbouring neurons modify their weight vectors so they also resemble the input signal, but less strongly, depending on their distance from the winner.

2.6 Group Method of Data Handling Neural Networks

One of the inherent problems of using ANN based algorithms in any domain is the potentially overwhelming choice of different architectures, network types, layer topologies and sizes. Rules-of-thumb, intuition or trial and error are often used as a means of choosing the type and structure of a network for a given problem, and this can lead to unnecessarily poor performance. The use of Group Method of Data Handling (GMDH) [51, 52] neural networks can assist users with these choices by automating many design decisions, reducing the need for *a priori* knowledge of the underlying model or system for the problem to be solved. GMDH neural networks have been applied to medical imaging of 3D heart images with some success [53], and have been used to select not only the neuron topology and network type, but also the input features to be used by the network. In [54] Kondo and Ueno applied a GMDH neural network to blood vessel image recognition, with automatic selection of an architecture from three distinct network types, further demonstrating the suitability of this approach for medical imaging. GMDH neural networks, like many approaches based on evolutionary or genetic algorithms, have the disadvantage of greater computational expense and less transparency. Solutions often require a large number of iterations of the training/searching algorithm, and for each additional degree of freedom (in terms of variables such as layer topology, architecture type etc.) the process takes longer to find a solution.

2.7 Neural Network and Medical Imaging Toolboxes

To assist readers with their efforts in reproducing and extending the works presented in this survey we provide a brief list of toolboxes for both neural networks and medical image analysis. This is by no means a comprehensive list, and is intended solely to present examples of available toolboxes that may be useful to readers of this survey.

One of the most well known toolboxes for constructing and training neural networks is the Neural Network Toolbox[1] for MATLAB. The toolbox provides GUIs for designing, training and simulating a number of different neural network types and allows custom extension of the toolbox. Fast Artificial Neural Network Library (FANN)[2] is a free cross-platform, open source toolbox for building and using neural networks. It provides bindings for many programming languages and third-party programs. Encog[3] is a framework for machine learning and neural network development. Supported in Java, .NET and Silverlight, it offers a comprehensive range of network architectures, training algorithms and neuron activation functions. Neuroph[4] is a free, open source framework for neural network development written using the Java programming language. While it offers less features than other toolboxes, it is lightweight, easy to use and can serve as a helpful introduction to creating neural networks.

[1] http://www.mathworks.com/products/neuralnet/
[2] http://leenissen.dk/fann/
[3] http://www.heatonresearch.com/encog
[4] http://neuroph.sourceforge.net/

The Medical Imaging Interaction Toolkit (MITK)[5] is a free and open source software system for visualising and processing medical images. It offers the possibility of integration with other applications and solutions, such as a neural network modelling implementation. ITK-SNAP[6] is another free and open source toolkit which provides support for semi-automatic and manual 3D image segmentation. ITK-SNAP and MITK are both based on the Insight Segmentation and Registration Toolkit (ITK)[7]. AMIDE[8] is a free tool for medical image analysis and registration that runs on a wide variety of platforms.

From the next section onwards, detailed descriptions are provided for computational intelligence in medical imaging with neural networks, and their applications over recent years are classified into four categories: registration, image segmentation and edge detection, computer aided diagnosis, and other applications. Each section gives more details on applications in one of these categories and overviews other relevant applications. Comparisons between neural networks applications are made in the concluding section.

3. Neural Networks for Medical Image Registration

Image registration is the process of transforming different sets of data into one coordinate system. Registration is necessary to enable the comparison, integration and fusion of images from different measurements, which may be taken at different points in time from the same modality or obtained from the different modalities such as CT, MR, Angiography and Ultrasound. Medical imaging registration often involves elastic (or non-rigid) registration to cope with elastic deformations of the body parts imaged, caused by changes from breathing, small movements or bodily changes over time. Non-rigid registration of medical images can also be used to register a patient's data to an anatomical atlas. Medical image registration is pre-processing step for many medical imaging applications and can have a strong influence on the result of subsequent segmentation and edge detection.

3.1 Techniques

Generally, image registration algorithms could be classified into two groups: area based methods and feature based methods. For area based image registration methods, the algorithm looks at the structure of the image via correlation metrics, Fourier properties and other means of structural

[5] http://www.mitk.org/wiki
[6] http://www.itksnap.org/
[7] http://www.itk.org/
[8] http://amide.sourceforge.net/

analysis. Most feature based methods fine tunes its mapping to the correlation of image features: lines, curves, points, line intersections, boundaries, etc.

To measure the volume change of lung tumour, Matsopoulos et al. [26] proposed an automatic three-dimensional non-rigid registration scheme that applied self-organizing maps (SOMs) to thoracic computed tomography (CT) data of patients for establishing correspondence between the feature points. The practical implementation of this scheme could provide estimations of lung tumour volumes during radiotherapy treatment planning. In the algorithm, the automatic correspondence of the interpolant points is based on the initialization of the Kohonen neural network model capable to identify 500 corresponding pairs of points approximately in the two CT sets S_1 and S_2. An overview of the described algorithm is illustrated in Figure 5.

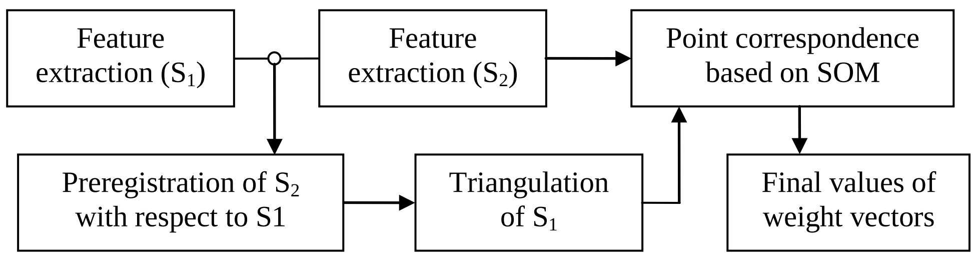

Figure 5 *The elastic registration scheme*

In the algorithm, two sets of points are defined: S_2 is the set of points for vertebrae, ribs and blades segmented from the reference data, and S_1 the set of points for the same anatomical structures from the second dataset called float data. Pre-registration takes place between these sets of points, and triangulation of S_1 is performed. The pre-registration process is applied in three dimensions and is applied in order to realign the two datasets in all coordinate. After pre-registration, two steps are performed to obtain the interpolant points, which are described below:

1. Triangulating S_1 and producing a wire frame based on the topology of S_1;

   The triangulation is based on Feitzke's work [27] and is performed by defining a SOM with the following characteristics:

   a. A grid of neurons with 20 rows by 100 columns (20 x 100) is chosen for the specific implementation.
   b. The initial weighting vectors of the neurons of the grid are set equal to the coordinates of a set of points extracted from an enclosing surface, typically a cylindrical surface.
   c. The input to the neural network consists of the Cartesian coordinates of the set of points that need to be triangulated.

After the process of adaptation of the neural network, the weighting vectors of the neurons have values identical to the appropriate points of S_1. A wire frame consisting of one node for each neuron can be constructed, with Cartesian coordinates of each node equal to the weight vector of the corresponding neuron. The wire frame is triangulated according to the connectivity of the neurons.

2. Establishing a SOM in terms of the topology of S_1 and training the SOM by using S_2;
   The search for corresponding points is based on replicating the topology of the set S_1 on the input layer of a SOM model. In the SOM model, one neuron is assigned to each node of the wired frame and the connections between the neurons are identical with the connections of the wired frame. No connection between two neurons is allowed if the two corresponding nodes are not directly connected on the float set. The initial weight vector of the neurons is the Cartesian co-ordinates of the corresponding wired frame nodes in the 3D space.

The training of the network is performed by presenting the network with the coordinates of randomly selected points sampled from the reference set S_2. The neuron with weight vector closest to signal is selected to fire. The firing neuron adjusts its weight vector and its neighbouring neurons modify their weight vectors as well but less strongly. The neighbouring neurons are confined to a window of 3 × 3 neurons throughout the network training.

The convergence of the SOM network during the triangulation of S_1 set of points results in a triangulated subset of points (S_1'). Each node of subset S_1' corresponds to a neuron of the SOM network (20 × 100 neurons), whose initial weighting vector (x_0,y_0,z_0) of S_1 is equal to the initial Cartesian coordinates of this node. In S_1, this node is displaced to new coordinates and equal to the final weighting vector (x_1,y_1,z_1). The new position always coincides with a point in S_2.

Although SOM lateral interactions between neurons generate a one to one point correspondence, more than one point from S1' may correspond to one point in S2. However, most of such point mismatches are avoided by using a distance threshold criterion that excludes corresponding points exceeding a distance more than five voxels. This process also prohibits excessive deformation of the final warped image. Therefore, the total number of successful corresponding points is reduced to approximately 500 pairs of points for all patient data.

SOM has also been used in many other registration-related applications. Shang et. al. [28] developed an automatic method to register computed tomography (CT) and magnetic resonance (MR) brain images by using first principal directions of feature images. In the method, principal component analysis (PCA) neural network is used to calculate the first principal directions from feature images, and then the registration is accomplished by simply aligning feature images' first principal directions and centroids.

Coppini [29] presented a general approach to the problem of image matching which exploits a multi-scale representation of local image structure. In the approach, a given pair of images to be matched, named target and stimulus respectively, are represented by Gabor Wavelets. Correspondence is computed by exploiting the learning procedure of a neural network derived from Kohonen's SOM. The SOM neurons coincide with the pixels of the target image and their weight are pointers to those of the stimulus images. The standard SOM rule is modified so as to account for image features.

Fatemizadeh et al. [30] proposed a method for automatic landmark extraction from MR brain images. In the method, landmark extraction is accomplished by modifying growing neural gas (GNG), which is a neural-network-based cluster-seeking algorithm. Using modified GNG (MGNG, a splitting-merging SOM) corresponding dominant points of contours extracted from two corresponding images are found. The contours are the boundaries of the regions generated by segmenting the MR brain image.

Di Bona et al. [31] developed the "Volume-Matcher 3D" project - an approach for a data-driven comparison and registration of three-dimensional (3D) images. The approach is based on a neural network model derived from self-organizing maps and extended in order to match a full 3D data set of a "source volume" with the 3D data set of a "target volume." In Zhang et al [55], an automatic surface-based rigid registration system using a neural network representation was proposed. The system was applied to register 3D volumes of human bone structures for image-guided surgery. A multilayer perceptron neural network was used to construct a patient-specific surface model from pre-operative images. A surface representation function derived from the resultant neural network model was then employed for intra-operative registration. The optimal transformation parameters were obtained via an optimization process. Experiments using image datasets of the calcaneus and vertebrae demonstrated that the segmentation/registration system could achieve sub-voxel accuracy comparable to that of conventional techniques, and was significantly faster.

Markaki et al. [56] proposed automatic point correspondence of unimodal medical images using Kohonen Network. Given a pair of 2D medical images of the same anatomical region and a set of interest points in one of the images, the algorithm detected effectively the set of corresponding points in the second image, by exploiting the properties of the Kohonen self organizing maps (SOMs) and embedding them in a stochastic optimization framework. The correspondences were established by determining the parameters of local transformations of point mapping in an iterative way, using a modified competitive learning as implemented by SOMs. Experimental results from three different modalities (CT, MR and red-free retinal images) had used to validate both the accuracy and efficiency of the proposed algorithm, even in the case of noise corrupted data. However, the proposed iterative solution was very time-consuming, and an execution time for an image pair was about 1-2 minutes. This became even worse when a more complex transform like affine was used.

3.2 Summary

Medical Image Registration is an important technique for comparing and linking multiple related images from different points in time. Small changes that can occur, such as from breathing or movement, require adaptive and flexible techniques that can successfully identify common points between multiple images. Herein there are two important criteria, i.e. the accuracy and the efficiency. Complex point correspondence model may appear very time-consuming, especially when estimation using iterative optimization is employed.

The ability of SOMs to organise their structures according to the topological arrangement of an input makes them well suited to image registration problems, where a SOM trained on a reference image can be applied to a second image. The mapping of input pixels from images, or other features if pre-processing has been performed, to output neurons in the SOM allows common features or points to be identified between both images. It is worth noting that combining the organisational ability of SOMs with other techniques can result in powerful registration algorithms. A Radial Basis Function was used in [26] as a warping method after the correlation between points in multiple images was found using a SOM. In [29] Coppini et al. discuss the use of Gabor Wavelets as an image representation technique, and note the need for appropriate data representation as dictated by the application and image content. Suitable pre-processing can improve the registration accuracy and aid in interpreting both final results as well as intermediate model states.

4. Neural Networks for Medical Image Segmentation and Edge Detection

Medical image segmentation is a process for dividing a given image into meaningful regions with homogeneous properties. Image segmentation is an indispensable process in outlining boundaries of organs and tumours and in the visualization of human tissues during clinical analysis. Therefore, segmentation of medical images is very important for clinical research, diagnosis, and applications, leading to requirement of robust, reliable and adaptive segmentation techniques. Image segmentation and edge detection often follows image registration and can serve as an additional pre-processing step in multi-step medical imaging applications. The following subsections describe applications of ANNs where segmentation or edge detection were the primary goals.

4.1 Segmentation

Kobashi et al. [15] proposed an automated method to segment the blood vessels from 3D time of flight (TOF) MRA volume data. The method consists of three steps: (1) removal of the background, (2) volume quantization, and (3) classification of primitives by using an artificial neural network.

After volume quantization by using a watershed segmentation algorithm, the primitives in the MRA image stand out. To further improve the result of segmentation, the obtained primitives have to been separated into the blood vessel class and the fat class. Three features and a feed-forward three-layered neural network are adopted for the classification. Compared with the fat, the blood vessel is like a tube - long and narrow. To this end, two features including vascularity and narrowness were introduced to measure such properties. As the histogram of blood vessels is quite different from that of the fat in shapes, a third feature, histogram consistency, is added for further improvement of the segmentation.

The feed-forward NN is composed of 3 layers: an input layer, a hidden layer and an output layer. The structure of the described neural network is illustrated in Figure 4.

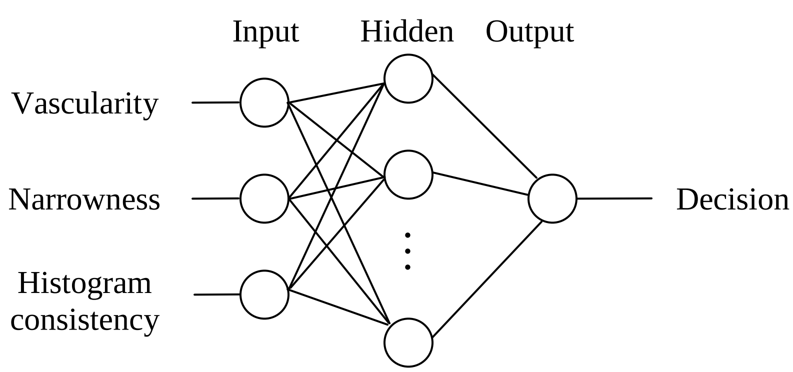

Figure 4 *Three layer feed-forward neural network*

As seen, three input units are included at the input layer, which is decided by the number of features extracted from medical images. The number of neuron in the output layer is one to produce and represent two classes. The number of neurons in the hidden layer is usually decided by experiments. Generally, a range of different numbers is tried in the hidden layer, and the number that achieves the best training results is selected.

In the proposed method, the ANN classifies each primitive, which is a clump of voxels, by evaluating the intensity and the 3D shape. In their experiments, the ANN was trained using 60 teaching data sets derived from an MRA data set. Each primitive is classified into the blood vessel (indicated by the value of 1) or the fat (indicated by the value of 0) and the values of the three features are calculated. All these values were fed into the feed-forward ANN for training the weights of the neurons. Seven new MRA data, whose primitives were unclassified, were fed into the trained NN for testing. The segmentation performance is measured by the value of accuracy as defined below, and the rate achieved by the reported algorithm is 80.8%.

$$Accuracy = \frac{Number\ of\ correctly\ classified\ primitives}{Total\ number\ of\ primitives} \times 100\% \qquad (4)$$

Apart from the work proposed by Kobashi in ANN based segmentation there are many applications for the images generated by CT and MRI. Middleton et al. [16] combined use of a MLP and active contour model ('snake') to segment structures in magnetic resonance (MR) images. The reported work can be highlighted by the following two steps: the perceptron is trained to produce a binary classification of each pixel as either a boundary or a non-boundary; subsequently, the resulting binary (edge-point) image forms the external energy function for a snake model, which is used to link the candidate boundary points into a continuous and closed contour.

Lin [17] applied a Hopfield neural network with penalized fuzzy c-means technique (called PFHNN) to medical image segmentation. In the algorithm, the pixels with their first and second order moments constructed from their *n* nearest neighbours as a training vector are mapped to a two-dimensional Hopfield neural network for the purpose of classifying the image into suitable regions.

Lin et al. [18] generalized Kohonen's competitive learning (KCL) algorithm with fuzzy and fuzzy-soft types called fuzzy KCL (FKCL) and fuzzy-soft KCL (FSKCL). These KCL algorithms fuse the competitive learning with soft competition and fuzzy c-means (FCM) membership functions. These generalized KCLs were applied to MRI and MRA ophthalmological segmentations. It is found that these KCL-based MRI segmentation techniques are useful in reducing medical image noise effects using a learning mechanism. The FSKCL algorithm is recommended for use in MR image segmentation as an aid to small lesion diagnosis.

Dokur [19] proposed a Quantizer Neural Network (QNN) for the segmentation of MR and CT images. QNN is a novel neural network structure, which is trained by genetic algorithms. It was comparatively examined with a multilayer perceptron and a Kohonen network for the segmentation of MR and CT head images. The QNN was reported to have the best classification performance with fewer neurons after a short training time.

Stalidis et al. [20] presented an integrated model-based processing scheme for cardiac magnetic resonance imaging (MRI), embedded in an interactive computing environment suitable for quantitative cardiac analysis, which provides a set of functions for the extraction, modelling, and visualization of cardiac shape and deformation. In the scheme, a learning segmentation process incorporating a generating-shrinking neural network is combined with a spatiotemporal parametric modelling through functional basis decomposition.

Chang et al. [21] developed an approach for medical image segmentation using a fuzzy Hopfield neural network based on both global and local gray-level information. The membership function simulated with neuron outputs is determined using a fuzzy set, and the synaptic connection weights between the neurons are predetermined and fixed to improve the efficiency of the neural network.

Shen et al. [22] proposed a segmentation technique based on an extension to the traditional fuzzy c-means (FCM) clustering algorithm. In the paper, a neighbourhood attraction, which is dependent on the relative location and features of neighbouring pixels, is shown to improve the segmentation performance and the degree of attraction is optimized by a neural-network model. Synthetic and real brain MR images with different noise levels are segmented to demonstrate the superiority of the proposed technique compared to other FCM-based methods.

Fu et al. [57] proposed an automatic hybrid model, in which the statistical expectation maximization (EM) and the spatial pulse coupled neural network (PCNN) were integrated for brain MRI segmentation. In addition, an adaptive mechanism was developed to fine tune the PCNN parameters. The EM model served two functions including evaluation of the PCNN image segmentation and adaptive adjustment of the PCNN parameters for optimal segmentation. They concluded the adaptive EM–PCNN yielded the best results for gray matter and brain parenchyma segmentation. However, the adaptive solution produced insignificant results in segmenting brain parenchyma in comparison with other solutions including non-adaptive EM–PCNN and EM, though it outperformed BCFCM in this test.

4.2 Edge Detection

Chang et al [23] designed a two-layer Hopfield neural network called the competitive Hopfield edge-finding neural network (CHEFNN) to detect the edges of CT and MRI images. The CHEFNN extends the one-layer 2-D Hopfield network at the original image plane to a two-layer 3-D Hopfield network with edge detection to be implemented on its third dimension. With the extended 3-D architecture, the network is capable of incorporating a pixel's contextual information into a pixel-labelling procedure. As a result, the effect of tiny details or noises will be effectively removed by the CHEFNN and the drawback of disconnected fractions can be overcome. In addition, they [24] discovered that high-level contextual information cannot be incorporated into the segmentation procedure in techniques using traditional Hopfield neural networks and thus proposed contextual constraint-based Hopfield neural cube (CCBHNC) for image segmentation. The CCBHNC uses a three-dimensional architecture with pixel classification implemented on its third dimension. With the three-dimensional architecture, the network is capable of taking into account each pixel's feature and its surrounding contextual information, achieving up to 95.86% segmentation accuracy on real MRI images. Recently, still for the edge detection, Chang [25] presented a special design Hopfield neural network called the contextual Hopfield neural network (CHNN). The CHNN maps the 2-D Hopfield network at the original image plane. With the direct mapping, the network is capable of incorporating pixels' contextual information into an edge-detecting procedure. As a result, the CHNN can effectively remove the influence of tiny details and noise.

In Suzuki et al [58], a neural edge detector (NED) is proposed to extract contours from left ventriculograms. A modified multilayer neural network is employed and trained using a modified back-propagation algorithm through supervised learning from a set of images with manually extracted edges by a cardiologist. It is found that the NED is able to extract the contours in agreement the ground truth, where an average contour error of 6.2% and an average difference between the ejection fractions at 4.1% are reported. However, how to deal with edges under severe noise and low contrast using techniques like active contour model needed to be further investigated.

4.3 Summary

Medical image segmentation and edge detection serve many useful purposes in medical imaging analysis. They can serve as a pre-processing step for further computer-aided diagnosis systems, or for human diagnosis. By classifying areas with similar properties more specialised diagnostic techniques can be applied with less risk of their misuse on non-relevant tissue. Identification of edges, particularly those of tumours and organs, can serve to simplify human diagnosis and reduce mistakes in the identification of image features.

The above sections describe a wide variety of different approaches, from various network types to a wide choice of feature extraction and pre-processing techniques. The commonly used network types include Hopfield, Kohonen, SOM, MLP, CNN, and QNN et al, where fuzzy c-means and fuzzy clustering along with genetic algorithm, EM, and BP algorithm are used for training. It is difficult to conclude, even in a general sense, which methodologies are consistently more appropriate than others. However, SOMs and contextual extension of conventional networks such as Hopfield net are often used in many different medical imaging applications due to their inherent topological mapping ability. Many imaging problems will require the topology of inputs, often in the form of raw pixel information or derived features, to be maintained through to the output stage, or at least clearly identifiable as a major component of the input-output mapping process. Other ANN approaches are, of course, still widely used. Their inherent differences can be mitigated for a single problem through careful data pre-processing or feature extraction/transformation. Hybrid or multipart systems can preserve the topology of inputs and produce derived features that are suitable for simpler network types such as MLPs. Still, when adopting a neural network solution choices are often dictated by the nature of the input data, or the desired form of output data. Simple numerical or nominal predictions may be more suited to a feed-forward or feed-back network, while solutions requiring spatial-based input and output might indicate a mapping network (such as a SOM) as a good starting point. In addition, it is useful to combine techniques like active contour model to achieve more robust image segmentation and contour extraction.

Although most of these applications are developed based on CT or MRI images, a wide variety of neural network types have been adopted for their analysis, and reported research results show extremely promising outcomes for both image segmentation and edge detection. Some ANNs are able to reduce the influence of noise in the image and hence make the segmentation more robust, making them a good choice where image noise is a significant problem. In many of the applications ANN approaches can be applied directly onto the images in question, greatly simplifying the analysis procedure. This must be balanced against potentially greater accuracies in systems where ANNs are applied to images that have been processed in some way, such as through background removal, feature extraction or dimensionality reduction.

5. Neural Networks for Computer Aided Detection, Diagnosis and Simulation

This section describes a number of applications where ANNs have been successfully used for computer aided diagnosis, detection and simulation. While each application is different, similarities derived from their common goals can be seen throughout this section. Neural networks have been incorporated into many computer-aided diagnosis systems, most of which distinguish cancerous signs from normal tissues. Generally these systems enhance the images first and then extract interesting regions from the images, possibly through segmentation and edge detection approaches such as those discussed in the previous section. The values of many features are calculated based on the extracted regions and are forwarded to neural networks that make decisions in terms of learning, training and optimizations. Among all applications, early diagnosis of breast cancers and lung cancers represents the most typical examples in the developed computer aided detection or diagnosis (CAD) systems. Some relevant survey papers can be found in [59, 60, 61].

5.1 Detection and Diagnosis of Breast Cancer using Digital Mammograms

Ge et al. [1] developed a computer-aided detection system to identify microcalcification clusters automatically on full field digital mammograms (FFDMs). The whole system includes six stages: pre-processing; image enhancement; segmentation of microcalcification candidates; false positive (FP) reduction for individual microcalcifications; regional clustering; and FP reduction for clustered microcalcifications.

To reduce FP individual microcalcifications, a convolution neural network (CNN) was employed to analysis 16×16 region of interest centred at the candidate derived from segmentations. CNN was designed to simulate the vision of vertebrate animals and can be considered as a simplified vision machine designed to perform the classification of the regions into two output types: disease and non-disease. Their CNN contains an input layer with 14 neurons, two hidden layers with 10 neurons each, and one output layer. The convolution kernel sizes of the first group of filters between the input and the first hidden layer were designed as 5×5, and those of the second group of filters between the first and second hidden layers were 7×7. The images in each layer were convolved with convolution kernels to obtain the pixel values to be transferred to the following layer. The logistic sigmoid function was chosen as the transfer function for both the hidden neurons and output neurons. An illustration of the neural network structure and its internal connections between the input layer, hidden layer and output layers is given in Figure 3.

The convolution kernels are organized in a way to emphasize a number of image characteristics rather than those less correlated values obtained from feature spaces for input. These characteristics include: (a) the horizontal versus vertical information; (b) local versus non-local information and (c) image processing (filtering) versus signal propagation [2].

The CNN was trained using back-propagation learning rule with the sum-of-squares error (SSE) function, which allows a probabilistic interpretation of the CNN output, i.e. the probability of correctly classifying the input sample as a true microcalcification ROI.

At the stage of FP reduction for clustered microcalcifications, morphological features (such as the size, the mean density, the eccentricity, the moment ratio, the axis ratio features and number of microcalcifications in a cluster) and features derived from the CNN outputs (such as the minimum, the maximum and the mean of the CNN output values) were extracted from each cluster. A total of 25 features (21 morphological features plus 4 CNN features) were extracted for each cluster. A linear discriminating analysis classifier was then used to differentiate clustered microcalcifications from false positives. The Stepwise LDA feature selection involves the selection of three parameters.

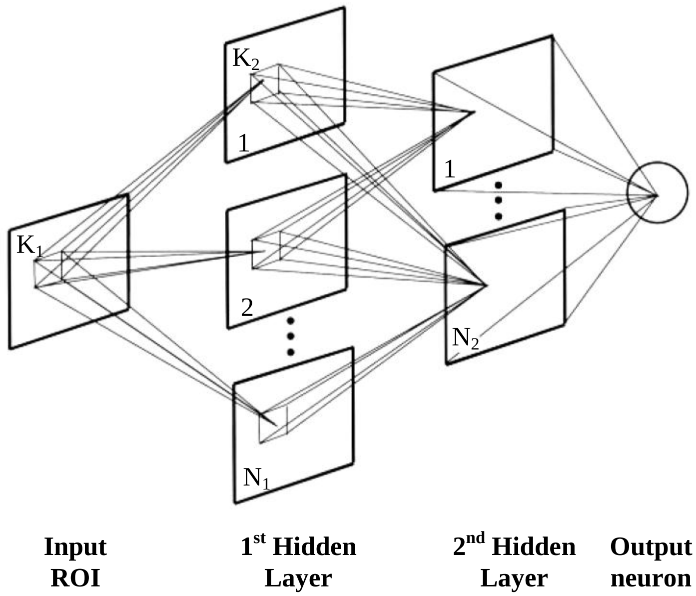

Figure 3 *Schematic diagram of a CNN*

In their study, a set of 96 images is split into a training set and a validation set, each with 48 images. An appropriate set of parameters is selected by searching in the parameter space for the combination of three parameters of LDA that could achieve the highest classification accuracy with a relatively small number of features in the validation set. Then the three parameters of LDA are used to select a final set of features and LDA coefficients by using the entire set of 96 training images which contain 96 TP and over 500 FP clusters. The trained classifier is applied to a test subset to reduce the false positives (FP) in the CAD system, and through ROC analysis was shown to achieve FP reduction rates of 86%, 74% and 72% at sensitivities of 70%, 80% and 90% respectively when compared to classification without the CNN/LDA approach.

To develop a computerized scheme for the detection of clustered microcalcifications in mammograms, Nagel et al. [3] examined three methods of feature analysis: rule based (the method currently used), an artificial neural network (ANN), and a combined method. The ANN method uses a three layer error-back-propagation network with five input units corresponding to the radiographic features of each microcalcification, and one output unit corresponding to the likelihood of being a microcalcification. The reported work reveals that two hidden units are insufficient for good performance of the ANN and it is necessary to have at least three hidden units to achieve adequate performances. However, the performance is not improved any further when the number of hidden units is increased over three. Therefore, the finalised ANN has five inputs, three hidden units, and one output unit. The hybrid approach incorporating both a rule-based classifier and an ANN achieved an error rate of 0.8 false positives per image at 83% sensitivity, compared to 1.9 and 1.6 for the rule-based method and the ANN alone respectively.

Papadopoulossa et al. [4] presented a hybrid intelligent system for the identification of microcalcification clusters in digital mammograms, which can be summarised in three-steps: (a) preprocessing and segmentation, (b) regions of interest (ROI) specification and (c) feature extraction and classification. In the classification schema, 22 features are automatically computed which refer either to individual microcalcifications or to groups of them. The reduction of false positive cases is performed using an intelligent system containing two subsystems: a rule-based and a neural network based. The rule construction procedure consists of the feature identification step as well as the selection of the particular threshold value for each feature. Before using the neural network, the reduction in the number of features is achieved through principal component analysis (PCA), which transforms each 22-dimensional feature vector into a 9-dimensional feature vector as the input to the neural network. The neural network that is used for ROI characterisation is a feedforward neural network with sigmoid hidden neuron (Multiplayer Perceptron—MLP).

In Halkiotis [62], ANN along with mathematical morphology is employed for the detection of clustered microcalcifications even under a non-uniform background. Considering each mammogram as a topographic representation, each microcalcification appears as an elevation constituting a regional maximum. Morphological filters are applied to suppress noise and regional maxima that do not correspond to calcifications. Two multi-layer perceptrons (MLP) and two radial basis function neural networks (RBFNN) with different number of hidden nodes are applied for classification. The MLP with ten hidden nodes achieved the best classification score with a true positive detection rate of 94.7% and 0.27 false positives per image.

Verma et al [63] proposed a soft cluster neural network (SCNN) for the classification of suspicious areas in digital mammograms. The idea of soft clusters was employed to increase the generalisation ability of ANN by providing a mechanism to more aptly depict the relationship between the input features and the subsequent classification as either a benign or malignant class.

Soft clusters with least square based optimisation made the training process faster and avoid iterative processes. The proposed neural network technique was tested on the DDSM benchmark database, and the accuracy achieved was over 93% in comparison with 83% from k-means clustering. However, the performance of the approach proposed was dependent on the properties of the sampled images and might fail if these conditions change including the optical density range of the film scanner and the spatial resolution of the mammograms.

Christoyiani et al. [5] presented a method for fast detection of circumscribed mass in mammograms employing a RBF neural network (RBFNN). In the method, each neuron output is a nonlinear transformation of a distance measure of the neuron weights and its input vector. The non-linear operator of the RBFNN hidden layer is implemented using a Cauchy-like probability density function. The implementation of RBFNN could be achieved by using supervised or unsupervised learning algorithms for an accurate estimation of the hidden layer weights. The K-means unsupervised algorithm is used to estimate the hidden-layer weights from a set of training data containing statistical features from both circumscribed lesions and normal tissue. After the initial training and the estimation of the hidden-layer weights, the weights in the output layer are computed by using Wincer-filter theory, or minimizing the mean square error (MSE) between the actual and the desired filter output. The method was tested using the The MIAS MiniMammiographic Database, and achieved a mean overlap value of 0.868 for true positives for both normal and abnormal mammograms.

Patrocinio et al. [6] demonstrate that only certain features such as irregularity, number of microcalcifications in a cluster, and cluster area, are needed as the inputs of a neural network to separate images into two distinct classes: suspicious and probably benign. Setiono [7] developed an algorithm by pruning a feed-forward neural network, which produces high accuracy rates for breast cancer diagnosis with small number of connections. The algorithm extracts rules from a pruned network by considering only a finite number of hidden unit activation values. Connections in the network are allowed only between input units and hidden units as well as between hidden units and output units. The algorithm finds and eliminates as many unnecessary network connections as possible during the training process. The accuracy of the extracted rules from the pruned network is almost as high as the accuracy of the original network.

The abovementioned applications cover different aspects of applying neural networks such as the number of neurons in the hidden layer, the reduction of features in classifications, the reduction of connections for better efficiency. Similar improvements could be made in applying ANN to other practical utilisations rather than just in identifying microcalcification clusters. For other approaches rather than ANN in detection and classification of microcalcifications and masses in mammograms, details can be found in [61] and [64].

5.2 Detection and Diagnosis of Lung Diseases

ANNs also plays an important role in detecting cancerous signs in lungs. Xu et al. [8] developed an improved computer-aided diagnosis (CAD) scheme for the automated detection of lung nodules in digital chest images to assist radiologists, who could miss up to 30% of the actually positive cases in their daily practice. In the CAD scheme, nodule candidates were selected initially by multiple gray-level thresholds of the difference image (subtraction of a signal-enhanced image and a signal suppressed image) and then classified into six groups. Between 50% and 70% of false positives were eliminated by adaptive rule-based tests and an ANN.

Zhou et al. [9] proposed an automatic pathological diagnosis procedure named Neural Ensemble-based Detection (NED) that utilizes an ANN ensemble to identify lung cancer cells in the specimen images of needle biopsies obtained from the bodies of the subjects to be diagnosed. An ANN ensemble is a learning paradigm where several ANNs are jointly used to solve a problem. The ensemble is built on a two-level ensemble architecture and the predictions of those individual networks are combined by plurality voting.

Keserci et al. [10] developed a computer-aided diagnosis scheme for automated detection of lung nodules in digital chest radiographs based on a combination of morphological features and the wavelet snake. In their scheme, an ANN was used to efficiently reduce false positives by using the combined features. The scheme was applied to a publicly available database of digital chest images for pulmonary nodules. Qian et al. [11] trained a computer-aided cytologic diagnosis (CACD) system to recognize expression of the cancer biomarkers histone H2AX in lung cancer cells and then tested the accuracy of this system to distinguish resected lung cancer from preneoplastic and normal tissues. The major characteristics of CACD algorithms are to adapt detection parameters according to cellular image contents. Coppini et al. [12] described a neural-network-based system for the computer aided detection of lung nodules in chest radiograms. The approach is based on multi-scale processing and feed-forward neural networks that allow an efficient use of a priori knowledge about the shape of nodules and the background structure.

5.3 Detection and Diagnosis in MRI

ANN has also been widely applied in diagnosis of diseases in MR images. In Guo et al [65], a computer-aided diagnostic system was proposed to classify rat liver lesions from MR imaging. Six parameters of texture characteristics and variance of 161 ROIs were calculated and assessed by gray-level co-occurrence matrices, then fed into a Back-Propagation neural network classifier to classify the liver tissue into two classes namely cirrhosis and HCC. The accuracy of classification of HCC nodules from cirrhosis achieved was 91.67%.

In Yamashita et al [66], ANN was utilised to evaluate the performance of radiologists for differential diagnosis of intra-axial cerebral tumours on MR Images. A single 3-layer feed-forward ANN with a Levenberg-Marquardt algorithm was employed to differentiate among 4 categories of tumours with the use of 2 clinical parameters and 13 radiologic findings in MR images. Subjective ratings for the 13 radiologic findings were provided independently by 2 attending radiologists. In total 126 cases were used for training and testing of the ANN based on a leave-one-out-by-case method. In the observer test, MR images were viewed by 9 radiologists, first without and then with ANN outputs. The averaged area under the ROC curve for ANN alone was 0.949. The diagnostic performance of the 9 radiologists increased from 0.899 to 0.946 when they used ANN outputs. However, the setup of the experiments was unrealistic as it might have introduced a bias into the results by telling observers that only 1 in 4 possible diseases were correctly diagnosed, with normal cases and other diseases excluded. As a result, the whole experiments seemed incomplete due to this reason as well as insufficient sample cases used to train and validate the ANN. Döhler et al [67] proposed a cellular ANN (CNN) for the detection of hippocampal sclerosis in MRI. Using an exemplary database that consisted of a large number of volumes of interest extracted from T1-weighted magnetic resonance images from 144 subjects, the authors demonstrated that the network allowed classifying brain tissue with respect to the presence or absence of mesial temporal sclerosis. Results indicated the general feasibility of the proposed computer-aided systems for diagnosis and classification of images generated by medical imaging systems. Due to the straightforward structural architecture of SNN that restricted itself to local couplings, hardware realizations of such networks were already available and offered the potentiality of real-time applications. However, this approach appear as a black box could hardly render an expert neuroradiologist "obsolete", since it did not provide information as to the origin of the obtained decision rule. In addition, at current stage it could only support T1-weighted volume scan, and further extension was needed to deal with T2 or FLAIR sequences when relevant high-resolution 3D-data became available.

In Bathen et al [68], multivariate models are proposed for the prediction of histological grade, hormone status, and axillary lymphatic spread in breast cancer patients. The multivariate methods applied are variable reduction by principal component analysis (PCA), and modelling by probabilistic neural network (PNN). Finally, the model is verified using prediction of blind samples. The verification results show that hormone status is well predicted by both PNN and PLS (partial least-squares regression) as a supplement for future clinical decision-making-concerning adjuvant treatment and the adaptation to more individualised treatment protocols. Although PNN produced satisfactory results in calibrating lymphatic spread from MR spectra in terms of sensitivity and specificity, predictions in blind samples were not as optimistic, which showed lack of generality of the proposed approach. In addition, more patients with less advanced breast cancer needed to be included in the test to balance the sample data for the feasibility testing the proposed method.

5.4 Functional MRI (fMRI) Simulation

Since the mid of 1990s, functional connectivity study using fMRI has drawn increasing attention of neuroscientists and computer scientists, which opens a new window to explore functional network of human brain [50]. Among quite a few work reported, ANN has been found as a natural way and powerful tool for simulating the connectivity and function of special areas of brain [47, 48, 69]. A comprehensive survey in this topic can be referred to in [49], [50] and [70].

In Kim and Horwitz [47], different kinds of fMRI functional connectivity are analysed to reflect the underlying interregional neural interactions, where a biologically realistic neural model is employed to simulate both neuronal activities and multiregional fMRI data from a blocked design. Topics involved include psycho-physiological interaction (PPI) analysis and interregional correlation analysis, and a large-scale neural model is applied to simulate the neurobiological underpinnings of PPI. The experimental results have clearly shown that neural modelling can be used to help validate the inferences one can make about functional connectivity based on fMRI data. However, the sensitivity of their findings could be a result of some artificial aspect of the attained neural model, such as the selection of 50% neurons in each region to be nonspecific in the task is arbitrary as the actual percentage of such neuron is unknown. The neural underpinnings of functional connectivity analysis for event-related fMRI designs and the adequacy of deconvolution in the neural model also needed to be further investigated.

In Marrellec et al [48], a novel approach based on the partial correlation matrix is proposed to develop data-driven measures of effective connectivity in functional MRI. To achieve this target, a large-scale, neurobiologically realistic neural network model is employed to generate simulated data with both structural equation modelling (SEM) and the partial correlation approach. Unlike real experimental data, where the interregional anatomical links are not necessarily known, the links between the nodes of the neural model are fully specified for easily judging the results of SEM and partial correlation analyses. The results reported have fully validated the partial correlation method with respect to the underlying neuroarchitecture. Since synthetic data were generated based on the comparison of SEM and partial correlation analysis with the true connectivity structure, this might be unrealistic thus the plotted shape of partial and marginal correlation coefficients and the proposed thresholding methods might lose of generality. Also it was unclear about the exact relationship between partial correlation and structural model analysis.

In Guenther et al [69], a neural model of speech acquisition and production is described that accounts for a wide range of acoustic, kinematic, and neuroimaging data concerning the control of speech movements. The components of the ANN model correspond to regions of the cerebral cortex and cerebellum, including premotor, motor, auditory, and somatosensory cortical areas. Computer simulations of the model verify its ability to account for compensation to lip and jaw perturbations during speech. Specific anatomical locations of the model's components are estimated, and these estimates are used to simulate fMRI experiments of simple syllable production. Although the described model accounted for most of the activity in fMRI study of speech production, it did not provide a complete explanation of the cortical and cerebellar mechanism involved such that better neural modelling and simulation could be achieved.

5.5 Detection and Diagnosis of Other Diseases

Apart from the applications in breast cancer and lung cancer, ANN has been adopted in many other analyses and diagnosis. Mohamed et al. [13] compare bone mineral density (BMD) values for healthy persons and identify those with conditions known to be associated with BMD obtained from Dual X-ray absorptiometry (DXA). An ANN was used to quantitatively estimate site-specific BMD values in comparison with reference values obtained by DXA (i.e. BMDspine, BMDpelvis, and BMDtotal). Anthropometric measurements (i.e. sex, age, weight, height, body mass index, waist-to-hip ratio, and the sum of four skinfold thicknesses) were fed to an ANN as independent input variables. The estimates based on four input variables were generated as output and were generally identical to the reference values for all studied groups.

Scott [14] tried determining whether a computer based scan analysis could assist clinical interpretation in this diagnostically difficult population. Artificial neural networks (ANNs) were created using only objective image-derived inputs to diagnose the presence of pulmonary embolism. The ANN predictions performed comparably to clinical scan interpretations and with the results of angiography.

In Chiu [45] et al, ANN model is employed for predicting skeletal metastasis in patients with prostate cancer. Through analysis of data consecutively collected from patients in five years, the predictors in terms of the patient's age and radioimmunometric serum PSA concentration are analysed. To assess the classification performance for clinical study, the discrimination and calibration of an ANN model is estimated and the one of the best performance is determined as four-layered perceptrons. Evaluations using the area under the receiver-operating characteristics curve and the Hosmer–Lemeshow statistics suggest that ANN appears to be a promising method in forecasting of the skeletal metastasis in patients with prostate cancer. However, the proposed model had several limitations including i) small number of patients enrolled, ii) single nuclear medicine physician used for interpretation of bone scintigraphic images, and iii) lack of a quantitative scale or scoring system for image interpretation. In addition, how to use PET/CT rather than scintigraphy for detecting skeletal metastasis also needed further attention.

In [71] Zhang et al. propose a computer-aided diagnosis system named LiverANN for classifying the pathologies of focal liver lesions into five categories using the artificial neural network (ANN) technique. On each MR image, a region of interest (ROI) in the focal liver lesion was delineated by a radiologist. The intensity and homogeneity within the ROI were calculated automatically, producing numerical data that were analyzed by feeding them into the LiverANN as inputs. Of the 320 MR images obtained from 80 patients with liver lesions, the ANN classifier can achieve a training accuracy of 100% and a testing accuracy of 93% in classifying the cases into five classes. Moreover, four kinds of MR imaging were considered including T1- and T2-weighted MR imaging, dynamic arterial phase and dynamic equilibrium phase.

Tägil et al [72] employed ANN for quality assurance of image reporting in terms of automatic interpretation in myocardial perfusion imaging. The networks were used to identify potentially suboptimal or erroneous interpretations of myocardial perfusion scintigrams (MPS). Reversible perfusion defects in each of 5 myocardial regions, as interpreted by one experienced nuclear medicine physician, were assessed by ANN in 316 consecutive patients undergoing MPS. After training, the ANNs were used to select 20 cases in each region that were more likely to have a false clinical interpretation. These cases, together with 20 detected control cases with no likelihood of false clinical interpretation, were randomly presented to three experienced physicians for a consensus re-interpretation. Due to small and mild perfusion defects and localization of defects, clinical routine interpretation by an experienced nuclear medicine expert and ANN differed in 53 of the 200 cases. The results demonstrated that ANN could identify those MPS that might have suboptimal image interpretations. However, the approach had two limitations. The first was that the processed images used for clinical interpretation and re-evaluation were nearly identical. The second was the lack of sufficient clinical information at the visual re-evaluation stage though such information was available at the clinical interpretation. Such difference might lead to different interpretation results in such a context.

In Pan et al [73], BP based ANN was utilised for bleeding detection in wireless capsule endoscopy (WCE). Colour texture features distinguishing the bleeding regions from non-bleeding regions were extracted in RGB and HSI colour spaces, and used as the feature vector inputs to the ANN to recognize the bleeding regions. The experiments demonstrated that the bleeding regions could be correctly recognized with a sensitivity of 93% and a specificity of 96%. However, inconsistent measurements in terms of sensitivity and specificity at 97% and 90% were also reported.

5.6 Summary

In all the computer aided diagnosis related applications mentioned above, the roles of ANNs have a common principle in the sense that they all are applied to reduce FP detections in both mammograms and chest images via examining the features extracted from the suspicious regions. Combining automatic detection of suspicious regions with human examination and diagnosis can significantly improve overall detection accuracy while minimising the amount of false negatives, as we can see from the reported research results. However, it is important to note that ANNs are not limited to academic research, but also play important roles in commercially available diagnosis systems. For example, R2 Technology's ImageChecker for mammograms was recently approved by the U.S. Food and Drug Administration for use in real-world diagnostic situations.

The main drawbacks of these approaches towards a successful CAD system can be found in several aspects including i) insufficient samples of patient, ii) lack of sufficient clinical information applied in diagnosis, iii) biased setting-up of the experiments, and iv) sensitive to imaging conditions. The imaging conditions here refer to how the images are produced, which can be image sequences from different sources (such as T1- and T2- weighted volume scan or FLAIR sequence in MRI) or differences in terms of spatial resolution and optical range of the film scanner. As a result, a practical system need to consider these issues in implementation the corresponding algorithms hence some multi-resolution analysis might help in this context, though it suffers high computational complexity.

According to the results reported in [46] and [64], it is interesting to note that combined classifiers tend to yield better results than single ones. However, ANN still can generate results as well as an expert mammographer, although in some work it is suggested that SVM may produce better results in detecting microcalcification. In Chen et al [74], it is found that the diagnostic performance of ANN is not different from that of SVM and LRA (Logistic regression analysis) as demonstrated by ROC curve analysis. The inconsistency here may refer to the differences between the test data and test conditions, i.e. how much of the data is used for training and how the classifiers are optimised.

6. Other Medical Applications using Neural Network

The preceding sections grouped together examples of ANN applications where a large domain existed, presenting multiple approaches for addressing similar medical image analysis problems. In this section a variety of ANN applications are presented that are not easy to categorise. It is hoped that this section may inspire readers to consider using ANNs for slightly less obvious tasks by showing how they have been successfully applied in the past. In addition to the areas mentioned above, ANN has also been applied to other relevant areas such as medical image compression [33-38], enhancement [39-44],, and tumour tracking [46].

6.1 Compression and Coding

Medical images, such as mammograms, are usually quite large in size and stored in databases inside hospital computer systems, which can present some difficulties in image transfer over the Internet. Image compression [32] attempts to alleviate these problems by reducing the size of medical images without losing important information. Some researchers have applied ANN to existing compression algorithms to select interesting regions for transmission or reduce the errors during the quantization in compression [33-37, 41].

Panagiotidis et al. [33] proposed a neural network architecture to perform lossy compression of medical images. To achieve higher compression ratio while retain the significant (from medical point of view) image content, the neural architecture adaptively selects regions of interest (ROI) in the images.

Karlik [34] presented a novel and combined technique for image compression based on the Hierarchical Finite State Vector Quantization (HFSVQ) and neural networks. The algorithm performs nonlinear restoration of diffraction-limited images concurrently with quantization. The neural network is trained on image pairs consisting of a lossless compression named hierarchical vector quantization.

Meyer-Base et al. [35] developed a method based on topology-preserving neural networks to implement vector quantization for medical image compression. The method can be applied to larger image blocks and represents better probability distribution estimation methods. The quantization process is performed by a "neural-gas" network which applied to vector quantization converges quickly to low distortion errors and reaches a distortion error lower than that resulting from Kohonen's feature map or the LBG algorithm. The influence of the neural compression method on the phantom features and the mammo-graphic image is not visually perceptible up to a high compression rate.

Jaiswal et al. [36] trained a resilient back propagation neural network to encode and decode the input data so that the resulting difference between input and output images is minimized. Lo et al [37] developed a neural-network-based framework to search for an optimal wavelet kernel that can be used for a specific image processing task. In the algorithm, a linear convolution neural network was employed to seek a wavelet that minimizes errors and maximizes compression efficiency for an image or a defined image pattern such as microcalcifications in mammograms and bone in computed tomography (CT) head images.

In Dokur [75], ANN was applied to medical images like magnetic resonance (MR), computer tomography (CT) head images and ultrasound imaging for compression and decision making, where Kohonen map and incremental self-organizing map (ISOM) were employed. In the proposed method, the image was first decomposed into blocks of 8×8 pixels, from which 2D discrete cosine transform (DCT) coefficients were computed. The dimension of the DCT coefficients vectors was reduced by low-pass filtering, a similar way like vector quantization. The decision making was realised simultaneously with compression to cluster codewords into several classes, which also formed a kind of segmentation of the original image. Higher compression rates with large signal to noise ratio were gained compared to the JPEG standard. Also it was found that ISOM generated better reconstructed images than Kohonen.

6.2 Image Enhancement and Noise Suppression

To enhance original images, ANN has been used to suppress unwanted signals such as noise and tissues affecting cancerous sign. Suzuki et. al. [38] proposed an analysis method that makes clear the characteristics of the trained NF (i.e. Nonlinear filters based on multilayer neural networks) and developed approximate filters that achieves very similar results but is efficient at computational cost.

To detect lung nodules overlapped with ribs or clavicles in chest radiographs, Suzuki et al. [39] developed an image-processing technique for suppressing the contrast of ribs and clavicles in chest radiographs by means of a multi-resolution massive training artificial neural network (MTANN). The structure of this neural network is illustrated in Figure 6, in which “bone” images are obtained by use of a dual-energy subtraction technique [40] as the teaching images to facilitate the neural network training. After that, the multi-resolution MTANN is able to provide “bone-image-like” images which are similar to the teaching bone images. By subtracting the bone-image-like images from the corresponding chest radiographs, they are able to produce “soft-tissue-image-like” images where ribs and clavicles are substantially suppressed.

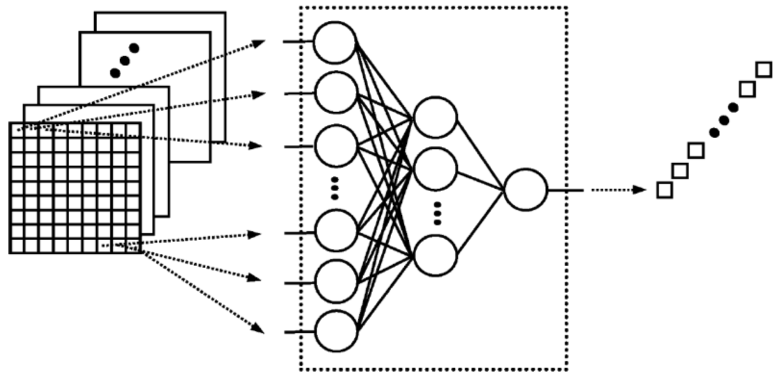

Figure 6 *Architecture of MTANN*

The MTANN consists of a linear-output multilayer ANN model, which is capable of operating on image data directly. The linear-output multilayer ANN model employs a linear function as the transfer function in the output layer because the characteristics of an ANN were improved significantly with a linear function when applied to the continuous mapping of values in image processing [41]. The inputs of the MTANN are the pixel values in a size-fixed sub-image and can be rewritten as $I_{x,y} = \{I_1, I_2, ..., I_N\}$, where N is the number of inputs i.e. the number of pixels inside a sub-image. The output of the nth neuron in the hidden layer is represented by

$$O_n = f_h\left\{\sum_{m=1}^{N} w_{mn} \cdot I_m - b_n\right\} \qquad (5)$$

Where w_{mn} is a weight between the m^{th} unit in the input layer and the nth neuron in the hidden layer, and f_h is a sigmoid function. The output of the neuron in the output layer is represented by:

$$f(x,y) = f_o\left\{\sum_{m=1}^{N_h} w_m^O \cdot O_m^H - b_o\right\} \qquad (6)$$

where $w^o{}_m$ is a weight between the m^{th} neuron in the hidden layer and the neuron in the output layer, b_o is an offset of the neuron in the output layer.

To train MTANN, a dual-energy subtraction technique is used to obtain the teaching image T (i.e. "bone" images) for suppression of ribs in chest radiographs. Input chest radiographs are divided pixel by pixel into a large number of overlapping sub-images. Each sub-image $I(x$,y) corresponds to a pixel $T(x, y)$ in teaching image, and the MTANN is trained with massive sub-image pairs as defined below:

$$\{I(x,y),T(x,y)|x,y \in R_T\} = \{(I_1,T_1),(I_2,T_2),\ldots,(I_{N_T},T_{N_T})\} \quad (7)$$

where R_T is a training region corresponding to the collection of the centres of sub-images, N_T is the number of pixels in R_T. After training, the MTANN is expected to produce images similar to the teaching images, i.e. "bone-image-like" images. The technique was evaluated using a set of 118 images by applying the algorithm to each image and then quantitatively comparing it to a dual-energy soft-tissue image where the bone regions had been deemphasised.

Since Ribs in chest radiographs include various spatial-frequency components and it is difficult in practice to train the MTANN with a large sub-image, multi-resolution decomposition/ composition techniques are employed in the algorithm. Three MTANNs for different resolutions are trained independently with the corresponding resolution images: a low-resolution MTANN is in charge of low-frequency components of ribs, a medium-resolution MTANN is for medium-frequency components, and a high-resolution MTANN for high-frequency components. After training, the MTANNs produce a complete high-resolution image based on the images with different resolution.

Hainc et al. [42] found the artificial neural network can also be used as a kind of a sophisticated non-linear filter on local pixel neighbourhood (3x3) since linear systems are not good in their sensitivity to impulse (isolated) noise.

Chen et al. [43] introduced an ANN architecture for reducing the acoustic noise level in magnetic resonance (MR) imaging processes. The proposed ANN consists of two cascaded time-delay ANN. The ANN is used as the predictor of a feedback active noise control (ANC) system for reducing acoustic noises. Preliminary results also show that, with the proposed ANC system installed, acoustic MR noises are greatly attenuated while verbal communication during MRI sessions is not affected.

6.3 Miscellaneous Applications

Apart from the categories of applications described above, ANN has been applied to medical image processing for other purposes. Wu et al. [44] presents a new method to extract the patient information number (PIN) field automatically from the film-scanned image using a multilayer cluster neural network. Cerveri et al. [76] presented a hierarchical radial basis function (HRBF) network to correct geometric distortions in X-ray image intensifier, which reduces the accuracy of image-guided procedures and quantitative image reconstructions.

Hsu et al. [77] establish a method to predict and create surface a profile of bone defects by a well-trained 3-D orthogonal neural network. The coordinates of the skeletal positions around the boundary of bone defects are input into the 3-D orthogonal neural network to train it to team the scattering characteristic. The 3-D orthogonal neural network avoids local minima and converges rapidly. After the neural network has been well trained, the mathematic model of the bone defect surface is generated, and the pixel positions are derived.

In Goodband et al. [46], application of ANN in image-guided radiation therapy is presented, aiming to improve the accuracy of treatment delivery by tracking tumour position and compensating for observed movement. Due to system latency it is sometimes necessary to predict tumour trajectory evolution in order to facilitate changes in beam delivery. A comparison is made between four different adaptive algorithms for training time-series prediction ANNs in analyzing optimized training and potential errors. A hybrid algorithm combining Bayesian regularization with conjugate-gradient backpropagation is demonstrated to give the best average prediction accuracy, whilst a generalized regression NN is shown to reduce the possibility of isolated large prediction errors. However, the four training algorithms proposed were used to train TSN NNs for tracking tumour movement, where it relied on external marker.

It is difficult to generalise all these applications of ANN into to several united models. However, it might be possible to analysis the general pattern of applying ANNs. In the next section, a comparison is made of the applications as described in all previous sections.

7. Discussions and Conclusions

As described in the previous five sections, applications of neural networks have been classified into four major categories. These applications seem quite different from each other and cover many aspects of medical image processing. The various different architectures available for medical imaging problems can present a dilemma for a prospective user. There are no rules or defined criteria that can be used to select the best network type, though the authors are confident that the examples presented throughout this paper will offer rules-of-thumb and guided inspiration for future efforts. To this end, all the neural networks successfully applied to medical imaging are highlighted and compared based on their application patterns, structures, operations, and training design etc. in Table 1. Since there is no theory nor compelling evidence to indicate a single “best” neural network approach for medical image processing and pattern recognition, the information such as “Type of Network”, "Type of input", "Number of Inputs", "Neurons in Hidden" and "Neurons in Output" is listed to help with searching and designing similar neural networks for the future applications. Although these applications may come from different areas such as CAD and segmentation, and inputs for neural networks are various, the essential purpose of applying these neural networks lies in their classifications, providing inspiring summary for existing modes of neural network applications and thus leading to further developments. Since the dataset for these applications are quite different, it is not possible to compare their results and the performance of these algorithms. The table does not cover all applications surveyed in this paper as information about numbers of neurons, layers, training and testing methodologies etc. were not always included in the referenced works.

In contrast to feed forward neural network, the applications of feedback neural networks for medical image processing are quite limited in the past decade and most of them are in the area of image segmentation, which are primarily based on Hopfield neural networks. The similarities between these applications are again limited but all of them need to minimise an energy function during convergence of the network. The energy function has to be designed individually, which might affect its application in medical imaging. Since the Hopfield neural network is unsupervised, it may not work for CAD like feed forward neural network that requires priori knowledge in classifications.

Although the applications of Kohonen's SOM are not as numerous as those of feed forward neural networks, its clustering and unsupervised properties make it very suitable for image registration. SOM converges to a solution that approximates its input data by adapting to prototype vectors. During this process, the relation of its neighbourhood neurons is also taken into account, leading to preservation of topology and mapping of training sets. This makes them particularly suitable for applications where dimensionality reduction is desirable and an output that can be easily interpreted is a necessary outcome. In this sense SOMs may be more suitable for certain applications than other neural network architectures, and other pattern recognition and classification approaches. For the applications of image registration, the input vectors of the neurons in SOM usually contain the spatial coordinate and intensity of pixels. For applications in image compression, SOM is used as a topology preserving feature map to generate vector quantization for code words. Sometimes, SOM produces the segmentation results for feed forward neural networks due to its unsupervised clustering property.

In summary, the applications of ANNs in medical image processing have to be analysed individually although many successful models have been reported in the literature. ANN has been applied to medical images to deal with the issues that can not be addressed by traditional image processing algorithms or by other classification techniques. By introducing artificial neural networks, algorithms developed for medical image processing and analysis often become more intelligent than conventional techniques. While this paper provided a focused survey on a range of neural networks and their applications to medical imaging, the main purpose here is to inspire further research and development on new applications and new concepts in exploiting neural networks.

Table 1 *Comparative summary of feed-forward neural network applications in medical imaging*

Source	Type of Network	Purpose	Type of Input	Number of Inputs	Neurons in Hidden layers	Neurons in Output	Train/Test /validation
[1]	CNN* /BP*	Detect FP*	Pixel intensity	256	14/10	1	268ROI*/267ROI
[3]	BP	Reduce FP	Value of features	5	5	1	1448 clusters/ leave-one-out
[4]	MLP*	Reduce FP	Value of features	9	20/10	1	Unknown
[5]	RBFNN*	Classify tissues	Value of features	4	5	2	44 regions /54 images
[8]	BP	Detect FP	Value of features	11	9	1	100 images / 100 images/ Jackknife[47]
[10]	BP	Detect FP	Value of features	10	5	1	397ROI/397 ROI/Jackknife
[12]	Feed-forward	Classify boundary	Coordinate /magnitude	3	30/10	1	100 images/ 147 images & 65 image CV
		Classify region	Coordinate /intensity	3	50	1	
[14]	BP	Predict tissue	Value of features	8	5	1	262/leave-one-out/Jackknife
				7	3	1	
[15]	BP	Classify tissues	Value of features	3	10	1	60 primitives /983 primitives
[20]	BP	Classify tissues	Statistical indexes	3	Unknown	3	Small number, improved by interaction
[22]	MLP	Classify boundary	Intensity of pixels	49	30	1	1200 patterns / 400 slices
[38]	BP	Remove noise	Intensity of pixels	25	20	1	Unknown
[39]	MTANN* (BP)	Classify tissues	Intensity of pixels	81	20	1	5000 Regions /118 images
[62]	MLP /RBFNN	Detect MCCs	intensity	5	10	1	107 RIO/ 19 images
[73]	BP	Classify & evaluation	Clinic & radiological findings	15	9	4	MR images of 126 cases, leave-one-out
[78]	BP	Classify MC	Value of features	14	13	1	100 ROI/ leave-one-out
[79]	MLBNN* (BP)	Classify MC	Vectors from SOM	5	25/14	7	32 cases/ 64 cases
[80]	BP	Classify tissues	Vectors from SOM	3	7	7	Unknown/ 80 images
[81]	BP	Detect Edge	Intensity of pixels	121	20	1	24 images/ fourfold CV

- BP: Back-propagation (feed forward)
- CNN: Convolution neural network
- CV: Cross validation
- FP: False positive MC or regions
- MC: Microcalcification cluster
- MLBNN: Multi-layered BP neural network
- MLP: Multiplayer perceptron
- RBFNN: Radial basis function neural network
- ROI: Region of interest
- SOM: Self-organizing map
- MTANN: Massive training ANN

While neural networks are undoubtedly powerful tools for classification, clustering and pattern recognition there are potential disadvantages when applying them to a given problem. Neural networks are notoriously hard to interpret and analyse, and in situations where it is desirable to simply and concisely define the process transforming inputs to output values it can be difficult to justify their use. While analysis of the internal weight and bias values for neurons in a network is possible, and a network itself can be represented formulaically, they are usually too large to be explained in a way that a human can easily understand. Despite this, they are still widely used in situations where a black-box solution is acceptable, and where empirical evidence of their accuracy is sufficient for testing and validation.

When compared to other machine learning approaches neural networks have many positive characteristics that must be considered by a prospective user. The variety of different network architectures and learning paradigms available, coupled with a theoretically limitless number of combinations of layers amounts, connections topologies, transfer functions and neuron amounts, make ANNs incredibly flexible processing tools. They can be applied to data with almost any number of inputs and outputs, and are well supported in different programming languages and software suites. Through manual modification of weights prior to training, and through imposing custom limitations on their modification during training, existing expert knowledge can be incorporated into their design and construction. Additionally, neural networks are usually computationally inexpensive to use after they have been trained, making them ideal for real-time applications where immediate output is desirable. Recent results suggest they can still generate comparable results to state-of-art classifiers like SVM [74].

Although this paper focuses on the various types of neural networks and how they can be applied to medical imaging, there are a variety of other approaches available for such an application. There are no clear rules or procedures that can be followed to determine if using a neural network is the best choice for a specific imaging problem, though guidance can be laid out to assist those that might consider their use. As discussed above, their inherent complexity makes them generally unsuitable for applications where post-training analysis of the way outputs are formed is necessary. In these situations there are clearly better choices of algorithm, such as decision trees, rule induction or Bayesian Networks where the impact that each input has upon the final result can be seen more clearly, and often in an inherently human-understandable way. However, neural networks unarguably possess strong potential for accurate output prediction, data clustering and topography-based mapping as can be seen by their widespread use in almost every discipline involving modelling and prediction.

References

1. J. Ge, B. Sahiner, L. M. Hadjiiski, H. P. Chan, J. Wei, M. A. Helvie, and C. Zhou, “Computer aided detection of clusters of microcalcifications on full field digital mammograms,” Medical Physics 33(8), pp: 2975-2988, 2006.
2. S. C. B. Lo, H. P. Chan, J. S. Lin, H. Li, M. T. Freedman and S. K. Mun, “Artificial convolution neural network for medical image pattern recognition”, Neural networks, 8(7-8), pp. 1201-11214, 1995
3. R. H. Nagel, R. M. Nishikawa, J. Papaioannou, and K. Doi, “Analysis of methods for reducing false positives in the automated detection of clustered microcalcifications in mammograms,” Medical Physics, 25(8), pp:1502-1506, 1998.
4. Papadopoulossa, D.I. Fotiadisb, A. Likasb, “An Automatic Microcalcification Detection System Based on a Hybrid Neural Network Classifier”, Artificial Intelligence in Medicine , pp: 149–167, v.25, 2002.
5. Christoyiani, E. Dermatas and G. Kokkinakis, “Fast Detection of Masses in Computer Aided Mammography”, IEEE Signal Processing Magazine, 17 (1), pp: 54–64, 2000.
6. A.C. Patrocinio, H. Schiabel, R.H. Benatti, C.E. Goes, and F.L.S. Nunes, “Investigation of clustered microcalcification features for an automated classifier as part of a mammography CAD scheme,” Proc. the 22nd Annual EMBS International Conf., July 23–28, 2000, pp. 1203–1205.
7. R. Setiono, “Extracting Rules from Pruned Neural Networks for Breast Cancer Diagnosis”, Artificial Intelligence in Medicine, 8(1), pp: 37–51, 1996.
8. X. W. Xu, K. Doi, T. Kobayashi, H. MacMahon, and M. L. Giger, “Development of an improved CAD scheme for automated detection of lung nodules in digital chest images,” Medical Physics, 24(9), pp.1395-1403, 1997.
9. Z. H. Zhou, Y. Jiang, Y. B. Yang and S. F. Chen, “Lung cancer cell identification based on artificial neural network ensembles,” Artificial Intelligence in Medicine, 24(1), pp:25-36, 2002.
10. B Keserci and H Yoshida, “Computerized detection of pulmonary nodules in chest radiographs based on morphological features and wavelet snake model,” Medical Image Analysis 6(4), pp:431-447, 2002.
11. Qian W, Zhukov T, Song DS and Tockman MS, “Computerized analysis of cellular features and biomarkers for cytologic diagnosis of early lung cancer,” Analytical and Quantitative Cytology and Histology, 29(2), pp:103-111, 2007.
12. G. Coppini, S. Diciotti, M. Falchini, N. Villari and G. Valli, “Neural networks for computer-aided diagnosis: Detection of lung nodules in chest radiograms,” IEEE Trans. Information Technology in Biomedicine, 7(4), pp: 344-357, 2003.
13. E. I. Mohamed, C. Maiolo, R. Linder, S. J. Poppl, and A. De Lorenzo, “Artificial neural network analysis: a novel application for predicting site-specific bone mineral density,” Acta Diabetologica, 40, pp: S19-S22, Suppl. 1, 2003.
14. J. A. Scott, “The lung scan and the abnormal chest X-ray: difficult diagnoses,” Nuclear Medicine Communications, 25(11), pp:1137-1141, 2004.
15. S. Kobashi, N. Kamiura, Y. Hata, and F. Miyawaki, “Volume-quantization-based neural network approach to 3D MR angiography image segmentation,” Image and Vision Computing, 19(4), pp:185-193, 2001.
16. Middleton and R. I. Damper, “Segmentation of magnetic resonance images using a combination of neural networks and active contour models,” Medical Engineering & Physics, 26(1), pp:71-86, 2004.
17. J. S. Lin, “Segmentation of medical images through a penalized fuzzy Hopfield network with moments preservation,” Journal of The Chinese Institute of Engineers, 23(5), pp:633-643, 2000.

18. K. C. R. Lin, M. S. Yang, H. C. Liu, J. F. Lirng and P. N. Wang, “Generalized Kohonen's competitive learning algorithms for ophthalmological MR image segmentation,” Magnetic Resonance Imaging, 21(8), pp:863-870, 2003
19. Z. Dokur and T. Olmez, “Segmentation of MR and CT images by using a quantiser neural network, Neural Computing & Applications,” 11(3-4), pp: 168-177, 2003.
20. G. Stalidis, N. Maglaveras, S. N. Efstratiadis, A. S. Dimitriadis and C. Pappas, “Model-based processing scheme for quantitative 4-D cardiac MRI analysis,” IEEE Trans. Information Technology In Biomedicine, 6(1), pp:59-72, 2002.
21. C. L. Chang and Y. T. Ching, “Fuzzy Hopfield neural network with fixed weight for medical image segmentation,” Optical Engineering, 41(2), pp:351-358, 2002.
22. S. Shen, W. Sandham, M. Granat, and A. Sterr, “MRI fuzzy segmentation of brain tissue using neighborhood attraction with neural-network optimization,” IEEE Trans. Information Technology In Biomedicine 9(3), pp:459-467, 2005.
23. C. Y. Chang and P. C. Chung, “Two-layer competitive based Hopfield neural network for medical image edge detection,” Optical Engineering, 39(3), pp:695-703, 2000.
24. C. Y. Chang and P. C. Chung, “Medical image segmentation using a contextual-constraint-based Hopfield neural cube,” Image and Vision Computing, 19(9-10), pp:669-678, 2001.
25. C. Y. Chang, “Contextual-based Hopfield neural network for medical image edge detection,” Optical Engineering, 45(3), Art. No. 037006, 2006.
26. G. K. Matsopoulosa, N. A. Mouravlianskya, P. A. Asvestasa, K. K. Delibasisa and V. Koulouliasb, “Thoracic non-rigid registration combining self-organizing maps and radial basis functions,” Medical Image Analysis, 9(3), pp. 237-254, 2005.
27. B. Fritzke, “A growing neural gas network learns topologies,” Advances in Neural Information Processing Systems 7, MIT press, Cambridge, MA, pp. 625-632, 1995.
28. L. F. Shang, J. C. Lv, and Z. Yi, “Rigid medical image registration using PCA neural network,” Neurocomputing, 69 (13-15), pp.1717-1722, 2006.
29. G. Coppini, S. Diciotti and G. Valli, “Matching of medical images by self-organizing neural networks,” Pattern Recognition Letters 25(3), pp.341-352, 2004.
30. E. Fatemizadeh, C. Lucas and H. Soltanian-Zadeh, “Automatic landmark extraction from image data using modified growing neural gas network,” IEEE Trans. Information Technology in Biomedicine, 7(2), pp:77-85, 2003.
31. S. Di Bona and O. Salvetti, “Neural method for three-dimensional image matching,” Journal of Electronic Imaging 11(4), pp:497-506, 2002.
32. J. Jiang, “Image compression with neural networks - A survey,” Image Communication, Journal of EURASIP, ELSEVIER, 14 (9), 1999.
33. N. G. Panagiotidis, D. Kalogeras, S. D. Kollias and A. Stafylopatis, “Neural network-assisted effective lossy compression of medical images,” Proceedings of the IEEE, 84(10), pp:1474 - 1487, 1996.
34. B Karlik, “Medical image compression by using vector quantization neural network (VQNN),” Neural Network World, 16 (4), pp.341-348 2006.
35. Meyer-Base, K. Jancke, A. Wismuller, S. Foo and T. Martinetz, “Medical image compression using topology-preserving neural networks,” Engineering Applications of Artificial Intelligence, 18(4), pp.383-392, 2005.
36. R. R. Jaiswal and A. N. Gaikwad, “Neural network assisted effective lossy compression of medical images,” IETE TECHNICAL REVIEW, 23 (2): 119-126, 2006.
37. S. C. B. Lo, H. Li, M. T. Freedman, “Optimization of wavelet decomposition for image compression and feature preservation,” IEEE Trans. Medical Imaging, 22(9), pp:1141-1151, 2003.
38. K. Suzuki, I. Horiba and N. Sugie, “Efficient Approximation of Neural Filters for Removing Quantum Noise from Images,” IEEE Trans. Signal Processing, 50(7), pp:1787-1799, 2002.

39. K. Suzuki, H. Abe, H. MacMahon and K. Doi, "Image-Processing Technique for Suppressing Ribs in Chest Radiographs by Means of Massive Training Artificial Neural Network (MTANN)," IEEE Trans. Medical Imaging, 25(4), 2006
40. K. Suzuki, I. Horiba, K. Ikegaya, and M. Nanki, "Recognition of coronary arterial stenosis using neural network on DSA system," Syst. Comput. Japan, vol. 26, no. 8, pp. 66–74, 1995.
41. K. Suzuki, "Neural edge enhancer for supervised edge enhancement from noisy images," IEEE Trans. Pattern Anal. Mach. Intell., vol. 25, no. 12,pp. 1582–1596, Dec. 2003.
42. L. Hainc and J. Kukal, "Role of robust processing in ANN de-noising of 2D image," Neural Network World, 16(2), pp:163-176, 2006.
43. G. K. Chen, T. D. Chiueh, J. H. Chen, "Active cancellation system of acoustic noise in MR imaging," IEEE Transactions On Biomedical Engineering, 46(2), pp:186-191, 1999.
44. H. H. P. Wu, "Patient information extraction in digitized X-ray imagery," Image and Vision Computing 22(3), pp:215-226, 2004.
45. J.-S. Chiu, Y.-F. Wang, Y.-C. Su, et al, "Artificial Neural Network to Predict Skeletal Metastasis in Patients with Prostate Cancer," Journal of Medical Systems, 33(2), pp. 91-100, April 2009.
46. J. H. Goodband, O. C. L. Haas, and J. A. Mills, "A comparison of neural network approaches for on-line prediction in IGRT," Med. Phys., 35(3), pp. 1113-1122, March 2008.
47. J. Kim and B. Horwitz, "Investigating the neural basis for fMRI-based functional connectivity in a blocked design: application to interregional correlations and psycho-physiological interactions," Magn Reson Imaging, 26(5), pp. 583-593, 2008.
48. G. Marrelec, J. Kim, J. Doyon, and B. Horwitz, "Large-Scale Neural Model Validation of Partial Correlation Analysis for Effective Connectivity Investigation in Functional MRI," Human Brain Mapping, 30(3), pp. 941-950, 2009.
49. S. J. Carrington and A. J. Bailey, "Are there theory of mind regions in the brain? A review of the neuroimaging literature," Human Brain Mapping, 30(8), pp. 2313-2335, 2008.
50. K. Li, L. Guo, J. Nie and T. Liu, "Review of methods for functional brain connectivity detection using fMRI," Computerized Medical Imaging and Graphics, 33(2), pp. 131-139, 2009.
51. S.J. Farlow, "The GMDH algorithm", In: S.J. Farlow, Editor, Self-organizing Methods in Modeling: GMDH Type Algorithms, Marcel Dekker, New York, pp. 1–24, 1984.
52. A. C. Ivakhnenko, "Polynomial theory of complex systems",IEEE Trans. Syst., Man, Cybernetics, pp. 364-378, Oct. 1971.
53. C. Kondo, T. Kondo and J. Ueno, "Three-dimensional medical image analysis of the heart by the revised GMDH-type neural network self-selecting optimum neural network architecture", Artificial Life and Robotics,14(2), pp:123-128, 2009.
54. T. Kondo and J. Ueno, "Multi-Layered GMDH-Type Neural Network Self-Selecting Optimum Neural Network Architecture and its Application to 3-Dimensional Medical Image Recognition of Blood Vessels", International Journal of Innovative Computing, Information and Control ICIC International, 4(1), pp. 175—187, 2008.
55. J. Zhang, Y. Ge, S. H. Ong, et al, "Rapid surface registration of 3D volumes using a neural network approach," Image and Vision Computing, 26(2), pp. 201-210, 2008.
56. V. E. Markaki, P. A. Asvestas, and G. K. Matsopoulos, "Application of Kohonen network for automatic point correspondence in 2D medical images," Computers in Biology and Medicine, 39(7), pp. 630-635, 2009.
57. J. C. Fu, C. C. Chen, J.W. Chai, et al, "Image segmentation by EM-based adaptive pulse coupled neural networks in brain magnetic resonance imaging," Computerized Medical Imaging and Graphics, In Press, 2010.
58. K. Suzuki, I. Horiba, N. Sugie, and M. Nanki, "Extraction of Left Ventricular Contours From Left Ventriculograms by Means of a Neural Edge Detector," IEEE Trans. Medical Imaging, 23(3), pp. 330-339, 2004.

59. P. J. Lisboa and A. F.G. Taktak, "The use of artificial neural networks in decision support in cancer: A systematic review," Neural Networks 19(4), pp. 408–415, 2006.
60. K. Doi, "Computer-aided diagnosis in medical imaging: Historical review, current status and future potential," Computerized Medical Imaging and Graphics, 31(4-5), pp. 198-211, 2007.
61. H. D. Cheng, X. Cai, X. Chen, L. Hu, and X. Lou, "Computer-aided detection and classification of microcalcifications in mammograms: a survey," Pattern Recog., 36(12), pp. 2967-2991, 2003.
62. S. Halkiotis, T. Botsis and M. Rangoussi, "Automatic detection of clustered microcalcifications in digital mammograms using mathematical morphology and neural networks," Signal Processing, 87(7), pp. 1559–1568, 2007.
63. B. Verma, P. McLeod and A. Klevansky, "A novel soft cluster neural network for the classification of suspicious areas in digital mammograms," Pattern Recog., 42(9), pp. 1845-1852, 2009.
64. H. D. Cheng, X. J. Shi, R. Min, L. M. Hu, X. P. Cai, and H. N. Du, "Approaches for automated detection and classification of masses in mammograms," Pattern Recog., 39(4), pp. 646-668, 2006.
65. D. Guo, T. Qiu, J. Bian, et al, "A computer-aided diagnostic system to discriminate SPIO-enhanced magnetic resonance hepatocellular carcinoma by a neural network classifier," Computerized Medical Imaging and Graphics, 33(8), pp. 588-592, 2009.
66. K. Yamashita, T. Yoshiura, H. Arimura, et al, "Performance Evaluation of Radiologists with Artificial Neural Network for Differential Diagnosis of Intra-Axial Cerebral Tumors on MR Images," American Journal of Neuroradiology, 29, pp.1153-1158, June-July 2008.
67. F. Döhler, F. Mormann, B. Weber, et al, "A cellular neural network based method for classification of magnetic resonance images: Towards an automated detection of hippocampal sclerosis," Journal of Neuroscience Methods, 170(2), pp. 324-331, 2008.
68. T. F. Bather, L. R. Jensen, B. Sitter, et al, "MR-determined metabolic phenotype of breast cancer in prediction of lymphatic spread, grade, and hormone status," Breast Cancer Research and Treatment, 104(2), pp. 181-189, 2007.
69. F. H. Guenther, S. S. Ghosh, and J. A. Tourville, "Neural modeling and imaging of the cortical interactions underlying syllable production," Brain and Language, 96(3), pp. 280-301, 2006.
70. A. E. Cavanna and M. R. Trimble, "The precuneus: a review of its functional anatomy and behavioural correlates," Brain, 129(3), pp. 564-583, 2006.
71. X. Zhang, M. Kanematsu, H. Fujita, et al, "Application of an artificial neural network to the computer-aided differentiation of focal liver disease in MR imaging," Radiological Physics and Technology, 2(2), pp. 175-182, 2009.
72. K. Tägil, J. Marving, M. Lomsky, et al, "Use of neural networks to improve quality control of interpretations in myocardial perfusion imaging," Int. J. Cardiovascular Imaging, 24(8), pp. 841-848, 2008.
73. G. Pan, G. Yan, X. Song and X. Qiu, "BP neural network classification for bleeding detection in wireless capsule endoscopy," J. Medical Engineering and Techno., 33(7), pp. 575-581, 2009.
74. S.-T. Chen, Y.-H. Hsiao,, Y.-L. Huang et al, "Comparative Analysis of Logistic Regression, Support Vector Machine and Artificial Neural Network for the Differential Diagnosis of Benign and Malignant Solid Breast Tumors by the Use of Three-Dimensional Power Doppler Imaging," Korean J. Radiol., 10(5), pp. 464–471, 2009.
75. Z. Dokur, "A unified framework for image compression and segmentation by using an incremental neural network," Expert Systems and Applications, 34(1), pp. 611-619, 2008.
76. P. Cerveri, C. Forlani, N. A. Borghese and G. Ferrigno, "Distortion correction for x-ray image intensifiers: Local unwarping polynomials and RBF neural networks," Medical Physics 29(8), pp:1759-1771, 2002.

77. J. H. Hsu and C. S. Tseng, "Application of three-dimensional orthogonal neural network to craniomaxillary reconstruction," Computerized Medical Imaging and Graphics 25(6), pp:477-482, 2001.
78. M. Kallergi, "Computer-aided diagnosis of mammographic microcalcification clusters," 31(2), Medical Physics, pp.314-326, 2004.
79. J.O. Glass, W. E. Reddick, O. Goloubeva, V. Yo and R.G. Steen, "Hybrid artificial neural network segmentation of precise and accurate inversion recovery (PAIR) images from normal human brain," MAGNETIC RESONANCE IMAGING, 18(10), pp:1245-1253, 2000.
80. W.E. Reddick, R.K. Mulhern, T.D. Elkin, J. O. Glass, T. E. Merchant and J. W. Langston, "A hybrid neural network analysis of subtle brain volume differences in children surviving brain tumors," MAGNETIC RESONANCE IMAGING, 16(4), pp.413-421, 1998.
81. K. Suzuki, I. Horiba, N. Sugie and M. Nanki, "Extraction of Left Ventricular Contours from Left Ventriculograms by Means of a Neural Edge Detector," IEEE Trans. Medical Imaging, 23(3), pp.330-339, 2004.